

Speech Dereverberation Using Non-negative Convolutional Transfer Function and Spectro-temporal Modeling

Nasser Mohammadiha, Simon Doclo

Abstract—This paper presents two single-channel speech dereverberation methods to enhance the quality of speech signals that have been recorded in an enclosed space. For both methods, the room acoustics are modeled using a non-negative approximation of the convolutional transfer function (N-CTF), and to additionally exploit the spectral properties of the speech signal, such as the low-rank nature of the speech spectrogram, the speech spectrogram is modeled using non-negative matrix factorization (NMF). Two methods are described to combine the N-CTF and NMF models. In the first method, referred to as the *integrated* method, a cost function is constructed by directly integrating the speech NMF model into the N-CTF model, while in the second method, referred to as the *weighted* method, the N-CTF and NMF based cost functions are weighted and summed. Efficient update rules are derived to solve both optimization problems. In addition, an extension of the integrated method is presented, which exploits the temporal dependencies of the speech signal. Several experiments are performed on reverberant speech signals with and without background noise, where the integrated method yields a considerably higher speech quality than the baseline N-CTF method and a state-of-the-art spectral enhancement method. Moreover, the experimental results indicate that the weighted method can even lead to a better performance in terms of instrumental quality measures, but that the optimal weighting parameter depends on the room acoustics and the utilized NMF model. Modeling the temporal dependencies in the integrated method was found to be useful only for highly reverberant conditions.

Index Terms—non-negative convolutional transfer function, spectral modeling, non-negative matrix factorization, speech dereverberation

I. INTRODUCTION

Recording a sound source in an enclosed space with a microphone placed at a distance from the sound source typically results in a signal that is reverberant, i.e., affected by the acoustic reflections against walls and objects within the enclosure. Reverberation may highly degrade the quality and intelligibility of speech [1], [2], and hence, in many speech communication applications, such as hearing aids, hands-free telephony, and automatic speech recognition, it is important to recover the (non-reverberant) clean speech signal [1].

Several methods have been developed for speech dereverberation, i.e., for estimating the clean speech signal from the

reverberant microphone signals. These methods can be broadly classified into spectral enhancement methods, probabilistic model-based methods, and acoustic multichannel equalization methods. Spectral enhancement methods [3]–[8] are usually designed to only suppress the late reverberation and are typically based on a room acoustic model parameterized by the reverberation time T_{60} and the direct-to-reverberation ratio (DRR). These methods first estimate the power spectral density (PSD) of the late reverberation, and then use spectral enhancement, e.g., Wiener filtering, to estimate the clean speech spectrogram. Probabilistic model-based methods [9]–[11] typically use an autoregressive process to model the reverberation, where the clean speech spectral coefficients are modeled using a Gaussian or a Laplacian distribution. Speech dereverberation is then performed blindly by estimating the unknown model parameters, including the reverberation model parameters and the clean speech spectral coefficients. Finally, in acoustic multichannel equalization methods, the room impulse responses (RIR) between the source and the microphones are blindly estimated and used to design an equalization system [12]–[14], where in theory perfect dereverberation can be achieved. However, multichannel equalization methods are only able to provide a good dereverberation performance if accurate estimates of the RIRs are available [15]. Although significant progress has recently been made, designing effective and robust speech dereverberation methods still remains a challenging task.

In this paper, we focus on single-channel dereverberation in the magnitude spectrogram domain. We assume that the magnitudes (or powers) of the short-time Fourier transform (STFT) coefficients of the reverberant signal at each frequency bin are obtained by convolving the STFT magnitudes (or powers) of the clean speech signal and the STFT magnitudes (or powers) of the RIR at that frequency bin [16], which is referred to as the non-negative convolutional transfer function (N-CTF) model hereafter. Although the N-CTF model only holds approximately, it can be advantageous as it does not require to model the RIR phase, which is difficult to be robustly modeled [16]. Recently, speech dereverberation methods based on this model have been proposed [16]–[20], which simultaneously estimate the power spectrograms of the clean speech signal and the RIR, where a sparsity constraint is usually imposed on each frequency bin of the speech spectrogram. Hence, since individual frequency bins are processed independently, these methods completely ignore the spectral structure of the speech signal. The main contribution of this paper is to propose blind

Nasser Mohammadiha has been with the Department of Medical Physics and Acoustics, University of Oldenburg, Germany, while working on this paper. He is currently with the Volvo Car Corporation, Sweden (e-mail: n.mohammadiha@gmail.com). Simon Doclo is with the Department of Medical Physics and Acoustics, University of Oldenburg, Germany (e-mail: simon.doclo@uni-oldenburg.de). This research was supported by the Cluster of Excellence 1077 Hearing4all, funded by the German Research Foundation (DFG).

single-channel speech dereverberation methods that jointly model the room acoustics using the N-CTF model and the speech spectrogram using non-negative matrix factorization (NMF).

NMF is a method to obtain a low-rank approximation of a non-negative matrix [21]. In speech processing, NMF is usually applied on the speech magnitude (or power) spectrogram, where the spectrogram is approximated by the product of two non-negative matrices, i.e., a basis matrix and an activation matrix. The basis matrix represents the repeating spectral patterns, while the activation matrix represents the presence of these patterns over time. As a result, it has been shown that NMF can be used to efficiently exploit the low-rank nature of the speech spectrogram and its dependency across the frequencies, and has been successfully applied for different problems in speech processing, e.g., [22]–[27].

In this paper, we present two methods to combine the N-CTF-based acoustic model and the NMF-based spectral model, resulting in two different cost functions. In the first method, referred to as the *integrated* method, the speech NMF model is integrated into the N-CTF model resulting in a combined cost function, while in the second method, referred to as the *weighted* method, the NMF- and N-CTF-based cost functions are weighted and summed. By minimizing the obtained cost functions, we derive new update rules to simultaneously estimate the spectrograms of the clean speech signal and the RIR. To additionally exploit the temporal dependencies of the speech signal (and hence spectro-temporal modeling of the speech signal) we use a frame-stacking method [26]. The estimated speech spectrogram is then used to compute a real-valued spectral gain in order to estimate the clean speech signal from the reverberant signal. It should be mentioned that while the proposed weighted method in this paper is novel, some preliminary results for the integrated method and modeling temporal dependencies have been discussed in [28]. In this paper, both dereverberation methods are compared with each other for several reverberant conditions, where we also investigate the dereverberation performance in the presence of background noise. For both dereverberation methods, the quality of the dereverberated signals is evaluated using three instrumental measures. Experimental results show that by additionally modeling the speech spectrogram using NMF in the N-CTF-based dereverberation, the instrumental speech quality measures substantially improve compared to the baseline N-CTF-based method, and that the proposed speech dereverberation methods outperform a state-of-the-art dereverberation method based on spectral enhancement [6]. Results indicate that the weighted method can lead to higher performance measures than the integrated method, but that the optimal weighting parameter between the NMF- and N-CTF-based cost functions depends on the room acoustics and the utilized NMF model. Finally, modeling the speech temporal dependencies using a frame-stacking method was only found to be useful for highly reverberant conditions when the low-rank NMF basis matrix was learned offline from clean speech training data.

The paper is organized as follows. The N-CTF model and its underlying assumptions are discussed in Section II. In

Section III a single-channel dereverberation method using the N-CTF model minimizing the generalized Kullback–Leibler divergence is reviewed. The dereverberation methods, combining the N-CTF and NMF models, are presented in Section IV and their performance is experimentally evaluated in Section V.

II. NON-NEGATIVE CONVOLUTIVE TRANSFER FUNCTION

We consider an acoustic scenario, where a single speech source is recorded using one microphone in a reverberant enclosure without background noise¹. Let $s(n)$ and $h(n)$ denote the discrete-time clean speech signal and the M -tap RIR between the speech source and the microphone, where n denotes the time index. The reverberant speech signal $y(n)$ is obtained by convolving $s(n)$ and $h(n)$, i.e.,

$$y(n) = \sum_{m=0}^{M-1} h(m) s(n-m). \quad (1)$$

In the STFT domain, (1) can be equivalently represented as [29]:

$$y_c(k, t) = \sum_{k'=1}^K \sum_{\tau=0}^{L_h-1} h_c(k, k', \tau) s_c(k', t-\tau), \quad (2)$$

where y_c , s_c , and h_c denote the complex-valued STFT coefficients of the microphone signal, the clean speech signal, and the RIR, k and k' denote the frequency index, K denotes the total number of frequency bins, t denotes the frame index, $t = 1, \dots, T$, and L_h denotes the RIR length in the STFT domain [29]. An approximation of (2), referred to as the convolutive transfer function (CTF), has been proposed in [30], where only band-to-band filters, i.e., $k = k'$, are used:

$$y_c(k, t) \approx \sum_{\tau=0}^{L_h-1} h_c(k, \tau) s_c(k, t-\tau), \quad (3)$$

where $h_c(k, k', \tau) = h_c(k, k, \tau)$ has been replaced with $h_c(k, \tau)$ for simplicity. Based on (3), it has been proposed in [16] to approximate the power spectrogram of the reverberant signal as (see Appendix A for details):

$$|y_c(k, t)|^2 \approx \sum_{\tau=0}^{L_h-1} |h_c(k, \tau)|^2 |s_c(k, t-\tau)|^2. \quad (4)$$

In this paper, we use a generalization of (4), i.e.

$$y(k, t) \approx \hat{y}(k, t) = \sum_{\tau=0}^{L_h-1} h(k, \tau) s(k, t-\tau), \quad (5)$$

where $y(k, t) = |y_c(k, t)|^p$, with $p = 1$ (magnitude spectrogram) or $p = 2$ (power spectrogram), and s and h are defined similarly as y . In (5), the spectrogram of the reverberant speech signal $y(k, t)$ is modeled as the convolution of the (non-negative) spectrogram of the clean speech signal $s(k, t)$ with non-negative coefficients $h(k, \tau)$ representing the acoustical environment, such that (5) is referred to as the non-negative convolutive transfer function (N-CTF) based acoustic model. Although (5) has been derived assuming $h(k, \tau) = |h_c(k, \tau)|^p$, it is important to note that in the remainder of the paper we will use the N-CTF model in (5) without necessarily relating

¹Please note that in Section V-B we will investigate the influence of background noise on the dereverberation performance.

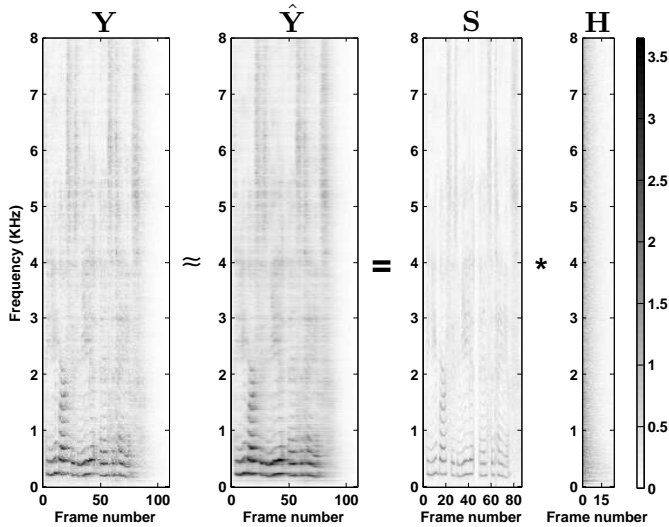


Fig. 1: N-CTF model approximation: The reverberant and clean speech magnitude spectrograms \mathbf{Y} and \mathbf{S} are obtained using an STFT with a frame length equal to 64 ms and 50% overlapping frames. \mathbf{H} is computed from a known RIR according to [29], where the off-diagonal elements have been set to zero. The N-CTF model in (6) is used to approximate \mathbf{Y} as $\hat{\mathbf{Y}} = \mathbf{S} * \mathbf{H}$.

the non-negative coefficients $h(k, \tau)$ to the time-domain RIR $h(n)$. In matrix notation (5) can be written as:

$$\mathbf{Y} \approx \hat{\mathbf{Y}} = \mathbf{S} * \mathbf{H}, \quad (6)$$

where $\mathbf{Y} = [y(k, t)]$ is a $K \times T$ -dimensional matrix, $\hat{\mathbf{Y}} = [\hat{y}(k, t)]$ is the resulting approximation for \mathbf{Y} , the $K \times (T - L_h + 1)$ -dimensional matrix \mathbf{S} and the $K \times L_h$ -dimensional matrix \mathbf{H} are defined similarly, and $*$ denotes a row-wise convolution of two matrices.

Fig. 1 shows an example to visualize the quality of the approximation for the N-CTF model when using $h(k, \tau) = |h_c(k, \tau)|$ to approximate the reverberant magnitude spectrogram \mathbf{Y} in (5), where a measured RIR ($T_{60} \approx 680$ ms, direct-to-reverberation ratio (DRR) around 0 dB) is used. The spectrogram \mathbf{Y} is computed by applying an STFT to $y(n)$ with a frame length equal to 64 ms and 50% overlapping frames (with a sampling frequency equal to 16 kHz). Similarly, the spectrogram \mathbf{S} is computed by applying an STFT to the clean speech signal $s(n)$. For the RIR, the representation from [29] resulting in $h_c(k, k', \tau)$ with $L_h = 24$ is first obtained, then the off-diagonal elements ($k \neq k'$) are set to zero and \mathbf{H} is computed as the magnitude of the resulting complex spectrogram. It has to be noted that computing \mathbf{H} by setting the off-diagonal elements of $h_c(k, k', \tau)$ to zero does not necessarily lead to the most accurate approximation of \mathbf{Y} in (6). Nevertheless, Fig. 1 shows that the N-CTF model, using the obtained \mathbf{H} , results in a quite good, albeit smooth, approximation of the reverberant spectrogram. In the following sections we will use the N-CTF model in (5) and blindly estimate both \mathbf{H} and \mathbf{S} to obtain the best approximation of the reverberant spectrogram \mathbf{Y} .

III. REVIEW OF DEREVERBERATION BASED ON THE N-CTF MODEL

The spectrogram of the clean speech signal $s(k, t)$ can be estimated by minimizing a cost function measuring the approximation error between the reverberant speech spectrogram $y(k, t)$ and its approximation $\hat{y}(k, t)$ in (5). As a cost function we will use the generalized Kullback-Leibler (KL) divergence [21] between y and \tilde{y} , which is a commonly used similarity measure to compare spectrograms, i.e.

$$Q = \sum_{k,t} KL \left(y(k, t) \left| \sum_{\tau=0}^{L_h-1} h(k, \tau) s(k, t - \tau) \right. \right), \quad (7)$$

where

$$KL(y(k, t) | \tilde{y}(k, t)) = y(k, t) \log \frac{y(k, t)}{\tilde{y}(k, t)} + \tilde{y}(k, t) - y(k, t). \quad (8)$$

The generalized KL divergence has been successfully applied for NMF-based speech enhancement and source separation [24], [26], [31], and has been used in [20] for dereverberation. In general, clean speech spectrograms can be assumed to be sparse, such that similarly to [16] it may be beneficial to add a sparsity-promoting term to (7), obtaining the regularized cost function:

$$Q = \sum_{k,t} KL \left(y(k, t) \left| \sum_{\tau=0}^{L_h-1} h(k, \tau) s(k, t - \tau) \right. \right) + \lambda \sum_{k,t} s(k, t), \quad (9)$$

where λ denotes the sparsity weighting parameter. Note that the cost function Q does not include any criterion on the structure of the speech spectrogram (except its sparsity), e.g., individual frequency bins are treated independently.

Under the non-negativity constraints $h(k, \tau) \geq 0$ and $s(k, t) \geq 0$, $s(k, t)$ and $h(k, \tau)$ can be estimated by minimizing the cost function in (9). By applying the iterative learning method using auxiliary functions, which is briefly reviewed in Appendix B, the following iterative update rules can be obtained for $h(k, \tau)$ and $s(k, t)$. Here, i denotes the iteration index, and $h^i(k, \tau)$ and $s^i(k, \tau)$ denote the estimates of $h(k, \tau)$ and $s(k, t)$ at the i -th iteration, respectively:

$$h^{i+1}(k, \tau) = h^i(k, \tau) \times \frac{\sum_t y(k, t) s^i(k, t - \tau) / \tilde{y}(k, t)}{\sum_t s^i(k, t - \tau)}, \quad (10)$$

$$s^{i+1}(k, t) = s^i(k, t) \times \frac{\sum_{\tau} y(k, t + \tau) h^{i+1}(k, \tau) / \tilde{y}(k, t + \tau)}{\sum_{\tau} h^{i+1}(k, \tau) + \lambda}, \quad (11)$$

where $\tilde{y}(k, t) = \sum_{\tau} h(k, \tau) s(k, t - \tau)$ is computed using the last available estimates of $h(k, \tau)$ and $s(k, t)$. To implement these update rules (and the ones in the next sections), a small positive number is typically added to the denominator to avoid division by zero. After convergence of the iterative learning method, the clean speech signal $s(n)$ is estimated using the estimated spectrogram $s(k, t)$ and inverse STFT, where the reverberant phase and the overlap-add procedure are used.

IV. DEREVERBERATION BASED ON ACOUSTIC AND SPECTRAL MODELS

To exploit a-priori knowledge about the speech spectrogram, e.g., the low-rank nature of the spectrogram and its structure across frequencies, we propose to add a spectral model of the clean speech signal to the acoustic model in (5). For this purpose, an NMF-based spectral model is introduced in Section IV-A. In the subsequent sections, two methods are presented to combine the N-CTF-based acoustic model in (5) with the NMF-based spectral model. These two methods exploit the NMF model in a different way, resulting in different cost functions and update rules. Section IV-B presents the integrated method, where the NMF model is directly integrated into the N-CTF model. In addition, an extension of the integrated method is described in Section IV-B which exploits temporal dependencies using a frame-stacking method. Section IV-C presents the weighted method, where the N-CTF- and NMF-based cost functions are weighted and summed.

A. NMF-based Spectral Model

Motivated by the successful modeling of speech spectrogram using non-negative matrix factorization (NMF) in different applications, we propose to use an NMF-based spectral model of the clean speech signal, i.e.,

$$s(k, t) \approx \sum_{r=1}^R w(k, r) x(r, t), \quad (12)$$

where $w(k, r)$ and $x(r, t)$ are both non-negative, and R denotes the number of basis vectors in the $K \times R$ -dimensional basis matrix $\mathbf{W} = [w(k, r)]$. In matrix notation, (12) can be written as $\mathbf{S} \approx \mathbf{W}\mathbf{X}$, where $\mathbf{S} = [s(k, t)]$ and $\mathbf{X} = [x(r, t)]$ denote the speech spectrogram and the activation matrix, respectively. R is typically chosen to be smaller than the dimensions of \mathbf{S} , so that (12) results in a low-rank approximation of \mathbf{S} .

Given a speech spectrogram \mathbf{S} , the basis matrix \mathbf{W} and the activation matrix \mathbf{X} can be estimated by minimizing a cost function measuring the distance between \mathbf{S} and $\mathbf{W}\mathbf{X}$. Common choices for the cost function are based on the generalized Kullback-Leibler (KL) divergence, the Euclidean distance, or the Itakura-Saito divergence. The obtained cost functions usually correspond to different probabilistic frameworks explaining how \mathbf{S} is generated given $\mathbf{W}\mathbf{X}$. For a given cost function, different optimization methods exist to iteratively estimate \mathbf{W} and \mathbf{X} , where typically gradient-descent update rules are applied for a number of iterations until a local minimum of the cost function has been reached. Multiplicative update rules are popular methods for this purpose, which are obtained for a particular choice of the step size in the gradient-descent update rules [21].

B. Integrated Method to Combine N-CTF and NMF

As the first method, we propose to directly integrate the NMF approximation of $s(k, t)$ in (12) into (5). Consequently, the following cost function is obtained [28]:

$$L_1 = \sum_{k,t} KL \left(y(k, t) \left| \sum_{\tau=0}^{L_h-1} h(k, \tau) \sum_{r=1}^R w(k, r) x(r, t - \tau) \right. \right) + \lambda \sum_{r,t} x(r, t), \quad (13)$$

where the sparsity constraint is now imposed on the activations x since s does not directly appear in (13). This helps to obtain sparse estimates for s , considering the relation between s and x in (12). The cost function in (9) is a special case of the cost function in (13) when the basis matrix \mathbf{W} is a $K \times K$ -dimensional identity matrix. Moreover, the cost function utilized in [20] is obtained as another special case, when \mathbf{W} is a fixed matrix.

To minimize (13), the iterative learning method using auxiliary functions from Appendix B can be used, leading to the following multiplicative update rules for h , w , and x :

$$h^{i+1}(k, \tau) = h^i(k, \tau) \frac{\sum_t y(k, t) \tilde{s}(k, t - \tau) / \tilde{y}(k, t)}{\sum_t \tilde{s}(k, t - \tau)}, \quad (14)$$

$$w^{i+1}(k, r) = w^i(k, r) \times \frac{\sum_{t,\tau} y(k, t) h^{i+1}(k, \tau) x^i(r, t - \tau) / \tilde{y}(k, t)}{\sum_{t,\tau} h^{i+1}(k, \tau) x^i(r, t - \tau)}, \quad (15)$$

$$x^{i+1}(r, t) = x^i(r, t) \times \frac{\sum_{k,\tau} y(k, t + \tau) h^{i+1}(k, \tau) w^{i+1}(k, r) / \tilde{y}(k, t + \tau)}{\sum_{k,\tau} h^{i+1}(k, \tau) w^{i+1}(k, r) + \lambda}, \quad (16)$$

where $\tilde{s}(k, t) = \sum_r w(k, r) x(r, t)$ and $\tilde{y}(k, t) = \sum_\tau h(k, \tau) \tilde{s}(k, t - \tau)$ are computed using the last available estimates of the parameters. These update rules can be efficiently implemented using the fast Fourier transform (FFT) [16]. To remove the scale ambiguity², after each iteration each column of \mathbf{W} is normalized to sum to one, and the columns of \mathbf{H} are element-wise divided by the first column of \mathbf{H} (resulting in an all-ones vector in the first column of \mathbf{H}). Moreover as suggested in [20], $h(k, \tau)$ is clamped to satisfy $h(k, \tau) < h(k, \tau - 1)$ for all τ .

Let $\hat{\mathbf{W}}$, $\hat{\mathbf{X}}$, and $\hat{\mathbf{H}}$ denote the obtained estimates after convergence of the iterative method. One possible estimate for the clean speech spectrogram \mathbf{S} is given by

$$\hat{s}(k, t) = \sum_{r=1}^R \hat{w}(k, r) \hat{x}(r, t). \quad (17)$$

Alternatively, the clean speech spectrogram can be estimated using a time-varying gain function as $\hat{s}(k, t) = G(k, t)y(k, t)$, where the gain function $G(k, t)$ is given by

$$G(k, t) = \frac{\sum_r \hat{w}(k, r) \hat{x}(r, t)}{\sum_{r,\tau} \hat{h}(k, \tau) \hat{w}(k, r) \hat{x}(r, t - \tau)}, \quad (18)$$

which was found to be particularly advantageous when the basis matrix \mathbf{W} was learned offline from speaker-independent clean speech training data. Since (17) directly uses the basis matrix to estimate the speech spectrogram, artifacts may be

²Note that if $\hat{\mathbf{H}}$, $\hat{\mathbf{W}}$, and $\hat{\mathbf{X}}$ are a solution to (13), the same value for L_1 can be obtained using $\alpha \hat{\mathbf{H}}$, $\hat{\mathbf{W}}/\alpha$, and $\hat{\mathbf{X}}$ for all non-negative numbers α .

Algorithm 1 Integrated method to combine N-CTF and NMF

Input : reverberant speech signal $y(n)$, output : dereverberated speech signal $\hat{s}(n)$

- 1) Set the model parameters: R (number of basis vectors), It (number of iterations), λ (sparsity parameter), L_h (RIR length in the STFT domain), and p (power).
 - 2) Initialize \mathbf{H}^1 , \mathbf{W}^1 and \mathbf{X}^1 with non-negative numbers (see Section V-A for more details).
 - 3) Compute the complex spectrogram $y_c(k, t)$ and the non-negative spectrogram $y(k, t) = |y_c(k, t)|^p$ by applying an STFT to $y(n)$.
 - 4) FOR $i = 1$ to It
 - a) Compute $\mathbf{H}^{i+1} = [h^{i+1}(k, \tau)]$ using (14)
 - b) Compute $\mathbf{W}^{i+1} = [w^{i+1}(k, r)]$ using (15)
 - c) Compute $\mathbf{X}^{i+1} = [x^{i+1}(r, t)]$ using (16)
- ENDFOR
- 5) Compute the time-varying gain function $G(k, t)$ using (18) and $h^{It}(k, \tau)$, $w^{It}(k, r)$, and $x^{It}(r, t)$.
 - 6) Compute the dereverberated speech signal $\hat{s}(n)$ by applying an inverse STFT and the overlap-add procedure to $\hat{s}_c(k, t) = G(k, t)^{1/p} y_c(k, t)$.

introduced, especially for unseen speakers. On the other hand, multiplying the reverberant spectrogram with the gain function in (18) only uses the basis matrix in an indirect way with $\hat{w}(k, r)$ appearing both in the nominator and denominator, leading to less artifacts. Algorithm 1 summarizes the integrated method.

The presented integrated method does not exploit temporal dependencies of the clean speech signal, i.e., consecutive frames are processed independently. Temporal dependencies are however an important aspect of speech signals and have been shown to be very beneficial for speech enhancement and source separation [24], [27], [32]. In order to investigate the benefit of modeling temporal dependencies for dereverberation, we propose an extension of the presented integrated method in Appendix C using the frame-stacking method [26]. In this method, a sliding window of size T_{st} frames is used to divide the speech magnitude spectrogram into a number of overlapping windows. All the consecutive frames within each window are then stacked to obtain a high-dimensional vector, using which a high-dimensional matrix is constructed. Finally, NMF is applied to the obtained high-dimensional matrix to learn a high-dimensional basis matrix, which contains both spectral and temporal information of the speech signal. This frame-stacking method is one of the important components in exemplar-based speech recognition [26]. In Section V, the integrated methods with and without modeling temporal dependencies are evaluated and compared.

C. Weighted Method to Combine N-CTF and NMF

Since both the N-CTF acoustic model in (5) and the NMF spectral model in (12) only hold approximately, it may be beneficial to be able to give different weights to the corresponding cost functions, which is not possible in the integrated method. This allows to give a larger weight to the more accurate

approximation. For the N-CTF acoustic model in (5) we can use the cost function in (9), whereas for the NMF spectral model in (12) we can use a similar cost function based on generalized KL divergence, i.e.

$$P = \sum_{k,t} KL \left(s(k, t) \left| \sum_r w(k, r) x(r, t) \right. \right) + \lambda \sum_{r,t} x(r, t), \quad (19)$$

where we have additionally used a sparsity-promoting term to encourage sparse estimates for the activations $x(r, t)$. The total cost function L_2 is now defined as the weighted sum of Q in (9) and P in (19):

$$L_2 = \rho P + (1 - \rho) Q, \quad (20)$$

where $0 < \rho < 1$ denotes the weighting parameter. Note that the same sparsity weighting parameter λ is used in P and Q as both sparsity constraints used in P and Q are related to the sparsity of the speech spectrogram (cf. (12)).

In the following, we use the iterative learning method using auxiliary functions from Appendix B to derive update rules to minimize L_2 w.r.t. h , s , w , and x . Here, we only derive the update rules for s since the update rules for the other parameters can be derived similarly. Let $L_2(s)$ denote all terms depending on s in (20), where h , w , and x are held fixed at h^i , w^i , and x^i , respectively:

$$L_2(s) = \rho \sum_{k,t} \left(s(k, t) \log \frac{s(k, t)}{\tilde{s}(k, t)} - s(k, t) \right) + (1 - \rho) \sum_{k,t} \left(\lambda s(k, t) + \sum_{\tau} h^i(k, \tau) s(k, t - \tau) \right) - (1 - \rho) \sum_{k,t} \left(y(k, t) \log \sum_{\tau} h^i(k, \tau) s(k, t - \tau) \right), \quad (21)$$

where $\tilde{s}(k, t) = \sum_r w^i(k, r) x^i(r, t)$. Minimizing $L_2(s)$ w.r.t. s can be solved using Theorem 1.

Theorem 1: The function $L_2(s)$ is non-increasing under the following update rule:

$$s^{i+1}(k, t) = \frac{-c(k, t)}{\rho \mathcal{W} \left(-\frac{c(k, t)}{\rho} e^{b(k, t)/\rho} \right)}, \quad (22)$$

where \mathcal{W} is the Lambert W function [33], which is defined as:

$$z = \mathcal{W}(z) e^{\mathcal{W}(z)}, \quad (23)$$

and

$$c(k, t) = -(1 - \rho) \sum_{\tau} \frac{y(k, t + \tau) s^i(k, t) h^i(k, \tau)}{\tilde{y}(k, t + \tau)}, \quad (24)$$

$$b(k, t) = (1 - \rho) \left(\sum_{\tau} h^i(k, \tau) + \lambda \right) - \rho \log \tilde{s}(k, t), \quad (25)$$

where $\tilde{y}(k, t) = \sum_{\tau} h^i(k, \tau) s^i(k, t - \tau)$.

Proof: Since $-\log(x)$ is a convex function, using Lemma 2 from Appendix B with $x_{\tau} = h^i(k, \tau) s(k, t - \tau)$ and $a_{\tau} =$

$h^i(k, \tau) s^i(k, t - \tau) / \tilde{y}(k, t)$, we can write:

$$\begin{aligned} & -\log \sum_{\tau} h^i(k, \tau) s(k, t - \tau) \leq \\ & -\sum_{\tau} \frac{h^i(k, \tau) s^i(k, t - \tau)}{\tilde{y}(k, t)} \log s(k, t - \tau) \\ & -\sum_{\tau} \frac{h^i(k, \tau) s^i(k, t - \tau)}{\tilde{y}(k, t)} \log \frac{\tilde{y}(k, t)}{s^i(k, t - \tau)}. \end{aligned} \quad (26)$$

Let us define the function $G(s, s^i)$ as:

$$\begin{aligned} G(s, s^i) &= \rho \sum_{k, t} \left(s(k, t) \log \frac{s(k, t)}{\tilde{s}(k, t)} - s(k, t) \right) + \\ & (1 - \rho) \sum_{k, t} \left(\lambda s(k, t) + \sum_{\tau} h^i(k, \tau) s(k, t - \tau) \right) - \\ & (1 - \rho) \sum_{k, t, \tau} \frac{y(k, t) h^i(k, \tau) s^i(k, t - \tau)}{\tilde{y}(k, t)} \log s(k, t - \tau) - \\ & (1 - \rho) \sum_{k, t, \tau} \frac{y(k, t) h^i(k, \tau) s^i(k, t - \tau)}{\tilde{y}(k, t)} \log \frac{\tilde{y}(k, t)}{s^i(k, t - \tau)}. \end{aligned} \quad (27)$$

Using (26) it can be shown that $L_2(s) \leq G(s, s^i)$. Since $G(s, s^i) = L_2(s)$, $G(s, s^i)$ is an auxiliary function for $L_2(s)$. Differentiating $G(s, s^i)$ w.r.t. $s(k, t)$ and rearranging the terms we obtain:

$$\frac{\partial G(s, s^i)}{\partial s(k, t)} = \frac{c(k, t)}{s(k, t)} + \rho \log s(k, t) + b(k, t), \quad (28)$$

where $c(k, t)$ and $b(k, t)$ are defined in (24) and (25), respectively. Defining $z(k, t) = -c(k, t) / (\rho s(k, t))$ and setting (28) equal to zero we obtain:

$$z(k, t) + \log z(k, t) = \log \left(-\frac{c(k, t)}{\rho} e^{b(k, t) / \rho} \right). \quad (29)$$

The solution to (29) is given by

$$z(k, t) = \mathcal{W} \left(-\frac{c(k, t)}{\rho} e^{b(k, t) / \rho} \right). \quad (30)$$

Substituting $z(k, t)$ with $-c(k, t) / (\rho s^{i+1}(k, t))$ leads to (22). The theorem is now proved using Lemma 1 from Appendix B. ■

In a similar way, the multiplicative update rules for w , x , and h can be derived as:

$$\begin{aligned} h^{i+1}(k, \tau) &= h^i(k, \tau) \times \\ & \frac{\sum_t y(k, t) s^{i+1}(k, t - \tau) / \tilde{y}(k, t)}{\sum_t s^{i+1}(k, t - \tau)}, \end{aligned} \quad (31)$$

$$\begin{aligned} w^{i+1}(k, r) &= w^i(k, r) \times \\ & \frac{\sum_t s^{i+1}(k, t) x^i(r, t) / \tilde{s}(k, t)}{\sum_t x^i(r, t)}, \end{aligned} \quad (32)$$

$$\begin{aligned} x^{i+1}(r, t) &= x^i(r, t) \times \\ & \frac{\sum_k s^{i+1}(k, t) w^{i+1}(k, r) / \tilde{s}(k, t)}{\sum_k w^{i+1}(k, r) + \lambda}, \end{aligned} \quad (33)$$

where $\tilde{s}(k, t)$ and $\tilde{y}(k, t)$, defined after (21) and (25), are computed using the last available estimates of the parameters. Algorithm 2 summarizes the proposed weighted method.

Algorithm 2 Weighted method to combine N-CTF and NMF

Input : reverberant speech signal $y(n)$, output : dereverberated speech signal $\hat{s}(n)$

- 1) Set the model parameters: R (number of basis vectors), It (number of iterations), λ (sparsity parameter), L_h (RIR length in the STFT domain), p (power), and ρ (weighting parameter).
- 2) Initialize \mathbf{H}^1 , \mathbf{S}^1 , \mathbf{W}^1 and \mathbf{X}^1 with non-negative numbers (see Section V-A for more details).
- 3) Compute the complex spectrogram $y_c(k, t)$ and the non-negative spectrogram $y(k, t) = |y_c(k, t)|^p$ by applying an STFT to $y(n)$.
- 4) FOR $i = 1$ to It
 - a) Compute $\mathbf{H}^{i+1} = [h^{i+1}(k, \tau)]$ using (31)
 - b) Compute $\mathbf{S}^{i+1} = [s^{i+1}(k, t)]$ using (22)
 - c) Compute $\mathbf{W}^{i+1} = [w^{i+1}(k, r)]$ using (32)
 - d) Compute $\mathbf{X}^{i+1} = [x^{i+1}(r, t)]$ using (33)

ENDFOR

- 5) Compute the time-varying gain function as

$$G(k, t) = \frac{s^{It}(k, t)}{\sum_{\tau=0}^{L_h-1} h^{It}(k, \tau) s^{It}(k, t - \tau)}. \quad (34)$$

- 6) Compute the dereverberated speech signal $\hat{s}(n)$ by applying an inverse STFT and the overlap-add procedure to $\hat{s}_c(k, t) = G(k, t)^{1/p} y_c(k, t)$.
-

V. EXPERIMENTAL RESULTS

This section presents the evaluation setup and the results of several experiments to evaluate the performance of the proposed single-channel speech dereverberation methods. Section V-A describes the acoustic setup, the used performance measures and the implementation details of the proposed methods, e.g., parameter values and initialization. Experimental results for the integrated method with and without temporal modeling are presented in Section V-B, where the performance of the integrated method is also compared to the performance of a state-of-the-art spectral enhancement method and the dereverberation performance in the presence of background noise is investigated. Section IV-C compares the performance of the integrated and weighted methods. Experimental results to analyze the effect of the parameters on the performance of the developed methods are described in Section V-D.

A. Evaluation Setup and Implementation Details

To evaluate the performance of the dereverberation methods for a wide variety of acoustic conditions, the reverberant microphone signals were generated by convolving clean speech signals with three different measured RIRs with reverberation times $T_{60} \approx 430$ ms, $T_{60} \approx 680$ ms, and $T_{60} \approx 640$ ms, and direct-to-reverberation ratios (DRR) around 5, 0, and 12 dB, respectively. As clean speech signals, 16 different sentences (uttered by 16 speakers) from the TIMIT database [34] were used to make the results independent of the speech material. The sampling frequency was 16 kHz and the STFT frame length and overlap length were equal to 64 ms and 32 ms,

respectively, where a square-root Hann window was used both for the STFT analysis and synthesis.

The dereverberation performance is evaluated using the following instrumental measures: the perceptual evaluation of speech quality (PESQ) [35] and the cepstral distance (CD) [36], both using the clean speech signal as the reference signal, and the reverberation decay tail (RDT) [37]. The RDT is defined as the ratio of the amplitude and decay rate of the exponential curves, which are fitted to the bark spectral difference between the reverberant and the clean signal, normalized to the amplitude of the direct component. A higher value for PESQ and a lower value for CD and RDT indicate a better performance. These measures exhibit a high correlation with subjective listening tests evaluating the quality of the dereverberated speech signals [38]. The *improvements* obtained in PESQ, denoted by ΔPESQ , and the *reductions* obtained in CD and RDT, denoted by ΔCD and ΔRDT , respectively, for the considered dereverberation methods are shown in the subsequent sections for better readability. To compute these differential scores, the score of the dereverberated signal is compared to the score of the reverberant microphone signal.

The proposed integrated and weighted methods are applied on the magnitude spectrogram of the reverberant microphone signals, i.e., $p = 1$, since using the magnitude spectrogram resulted in a better dereverberation performance compared to the power spectrogram (cf. Section V-D). For both integrated and weighted methods, two different ways were used to learn the basis matrix \mathbf{W} :

- The basis matrix \mathbf{W} , with $R = 100$ columns, was estimated from the reverberant speech signal. These variants are referred to as N-CTF+NMF and N-CTF+NMF (w), respectively, where the suffix '(w)' is used throughout the experiments to indicate the weighted method.
- The basis matrix \mathbf{W} was learned offline from clean speech training data, consisting of 250 sentences uttered by 27 speakers, disjoint from the test data, and was held fixed in the experiments. We consider two types of speaker-independent NMF models: 1) a low-rank NMF model with $R = 100$ (N-CTF+NMF+LR), and 2) an overcomplete NMF model with $R = 3000$ (N-CTF+NMF+OC). The basis matrix of this overcomplete model was constructed by sampling from the magnitude spectrogram of the training data using a uniform random walk method [39].

The RIR length in the STFT domain L_h was set to 10, corresponding to 320 ms, independent of the reverberation time. Each row of \mathbf{H} was initialized identically using a linearly-decaying envelope, while \mathbf{W} and \mathbf{X} were first initialized by random non-negative numbers and then updated by iterating the standard NMF update rules on the spectrogram of the reverberant signal \mathbf{Y} for 10 times. For the weighted method, \mathbf{S} was initialized with \mathbf{Y} . The T_{st} parameter in the frame-stacking method to model the temporal dependencies was set to 6. For both methods, the sparsity parameter λ was set to $\frac{0.1}{KT} \sum_{k,t} y(k,t)$ and to encourage sparser solutions, after each iteration the estimates of x and s were raised to a power ϕ_x as proposed in [40]. The maximum number of iterations was

experimentally set to 20 for the integrated method and 70 for the weighted method.

The proposed methods are compared to the baseline N-CTF method (cf. Section III), which does not use any spectral model, and a state-of-the-art speech spectral enhancement method, where the late reverberant spectral variance was estimated using [6] based on *oracle* T_{60} and DRR values computed from the RIR, and the log-spectral amplitude estimator [41] was used to estimate the clean speech STFT coefficients; this method is referred to as the SE method in the following. It should be noted that the N-CTF-based dereverberation methods including the proposed methods are batch methods, i.e., the whole reverberant microphone signal corresponding to a short utterance is used to estimate the clean speech signal, while the SE method using [6] is an on-line method. Developing an on-line N-CTF-based dereverberation method, similar to on-line NMF-based speech enhancement such as [27] remains a question for future research.

B. Integrated Method

Fig. 2 depicts exemplary spectrograms (for the RIR with $T_{60} \approx 680$ ms and $\text{DRR} \approx 0$ dB) of the noiseless reverberant and clean speech signals together with the spectrograms of the dereverberated speech signals using the proposed N-CTF+NMF+OC method and the SE method. As can be observed, reverberation effects have been substantially reduced using the proposed method.

To quantitatively compare the dereverberation performance in the absence of background noise, ΔPESQ , ΔCD , and ΔRDT values obtained using several variants of the integrated method, averaged over the 16 speech utterances, are shown in Fig. 3, Fig. 4, and Fig. 5 for the three considered RIRs. Also, Fig. 6 shows the average results over all 48 test utterances (3 RIRs and 16 speech utterances per RIR). In all figures, the suffix '(t)' is used to indicate that the methods use the temporal dependencies. Several conclusions can be drawn by studying these results:

1) *Using NMF-based spectral model in N-CTF*: By additionally using an NMF-based spectral model, i.e., using the N-CTF+NMF method, the performance of the N-CTF-based dereverberation method substantially improves for all RIRs. A consistent improvement is observed for all three measures for all considered RIRs using the N-CTF+NMF method compared to the N-CTF method.

2) *N-CTF-based methods versus spectral enhancement method*: The dereverberation method using only the N-CTF model leads to a higher ΔCD but a lower ΔRDT compared to the spectral enhancement (SE) method, which implies that the N-CTF method introduces less distortion but also leaves more late reverberation in the dereverberated speech signals. Considering PESQ, which evaluates the overall speech quality, the N-CTF method results in slightly better scores compared to the SE method. The proposed N-CTF+NMF method outperforms the SE method for all considered RIRs and instrumental measures. For example, the proposed N-CTF+NMF method outperforms the SE method by more than 0.25 PESQ-MOS points for all considered RIRs.

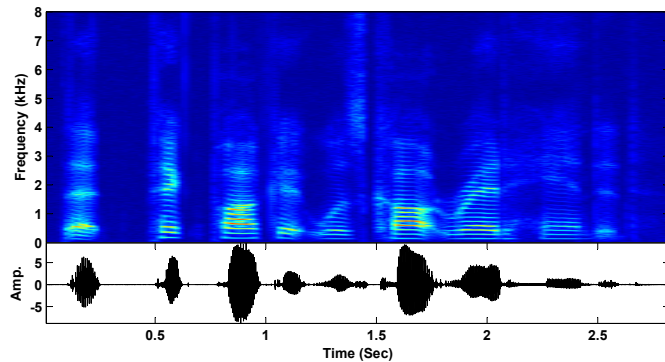
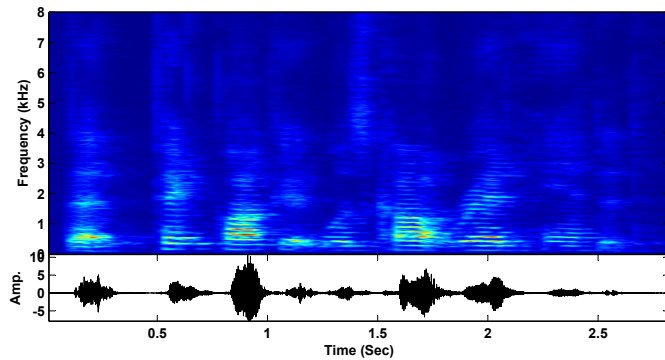
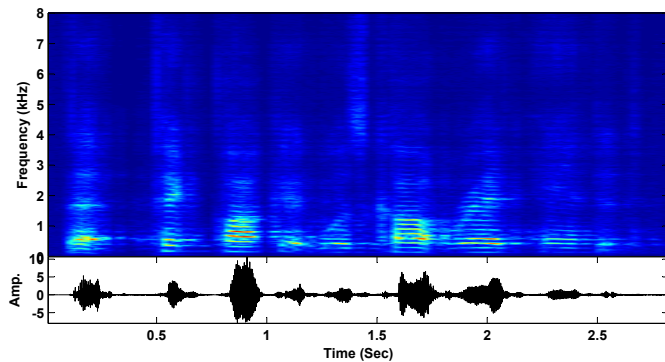
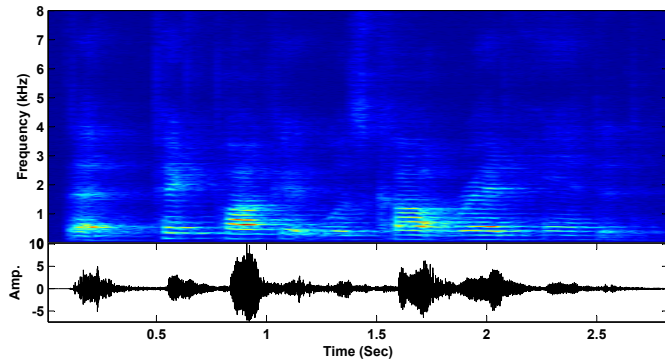


Fig. 2: Spectrograms of (a) reverberant microphone signal, (b) dereverberated signal using N-CTF+NMF+OC, (c) dereverberated signal using spectral enhancement (SE), (d) clean speech signal ($T_{60} \approx 680$ ms and $DRR \approx 0$ dB).

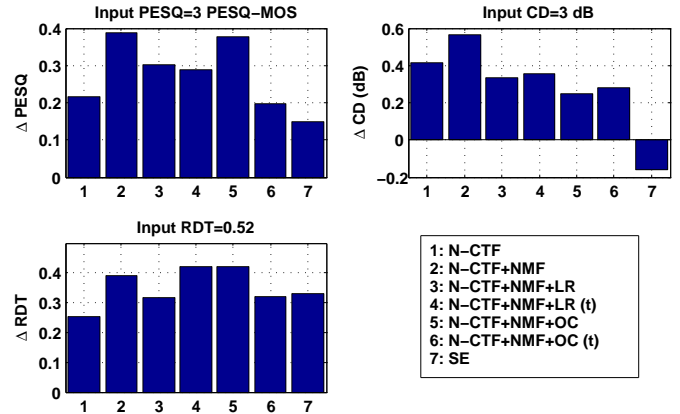


Fig. 3: Instrumental measures for the proposed methods for a RIR with $T_{60} \approx 640$ ms and $DRR \approx 12$ dB.

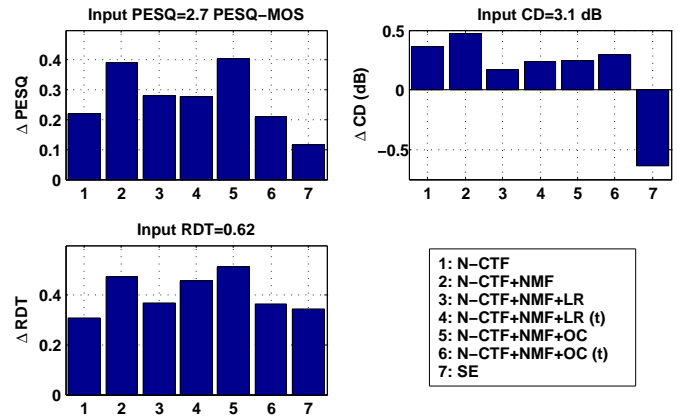


Fig. 4: Instrumental measures for the proposed methods for a RIR with $T_{60} \approx 430$ ms and $DRR \approx 5$ dB.

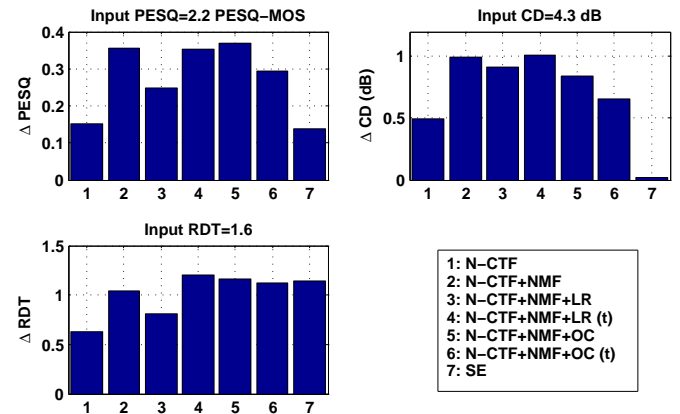


Fig. 5: Instrumental measures for the proposed methods for a RIR with $T_{60} \approx 680$ ms and $DRR \approx 0$ dB.

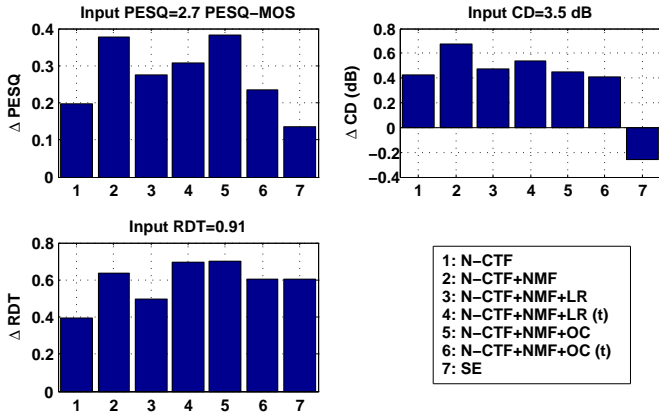


Fig. 6: Instrumental measures for the proposed methods, averaged over the three considered RIRs.

3) *Offline- versus online-learned basis matrices:* The results consistently show that the performance of the N-CTF+NMF+LR method with $R = 100$ offline-learned basis vectors is worse than the performance of the online counterpart N-CTF+NMF. However, by using a larger basis matrix with $R = 3000$ offline-learned basis vectors (N-CTF+NMF+OC) the performance improves and is comparable to the performance of the N-CTF+NMF method. Both these methods result in comparable Δ PESQ scores; the N-CTF+NMF+OC method results in a lower Δ CD but a higher Δ RDT compared to the N-CTF+NMF method. This can be explained by the fact that in the N-CTF+NMF+OC method the NMF basis matrix is learned offline using speaker-independent training data and is held fixed. This may lead to some artifacts in the dereverberated speech signal due to the mismatch between training and testing data. At the same time, since the basis matrix is held fixed, the model is able to better separate the reverberant component from the clean component, which leads to a larger reduction of the reverberant tail.

4) *Using temporal dependencies:* The experiments show that modeling the temporal dependencies using the frame-stacking method only appears to be useful for highly reverberant conditions when the N-CTF+NMF+LR method is used. As can be seen in Fig. 5, using the temporal dependencies in the N-CTF+NMF+LR method (i.e., the N-CTF+NMF+LR (t) method) leads to an additional improvement in the instrumental measures. By using the temporal dependencies the reverberant tail is significantly reduced but the cepstral distance is not changed noticeably. However, for the N-CTF+NMF+OC method, no improvement is observed by additionally using the temporal dependencies (i.e., using the N-CTF+NMF+OC (t) method). It should be mentioned that the N-CTF+NMF (t) method (not shown in the figures) resulted in a similar performance as the N-CTF+NMF method, and hence it is omitted in the figures for readability.

The experimental results shown in Fig. 3-6 are obtained without considering any background noise. To investigate the robustness of the proposed dereverberation methods to the presence of background noise, experiments were performed where speech-shaped noise was added to the reverberant mi-

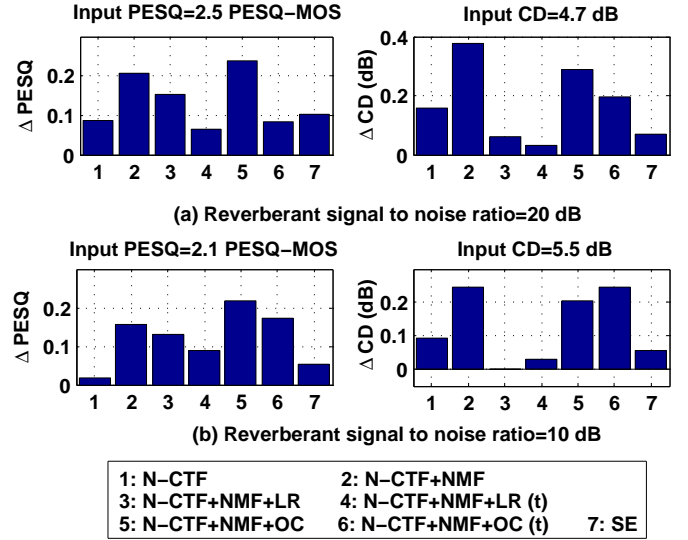


Fig. 7: Instrumental measures for the proposed methods for two background noise levels, averaged over the three considered RIRs.

crophone signals at two reverberant-signal-to-noise ratios (10 dB and 20 dB). Fig. 7 shows the average Δ PESQ and Δ CD values over all 48 test utterances. Due to space limitation, results for individual RIRs are not shown in the paper. It should be noted that due to the presence of background noise the input PESQ and CD scores are lower in this figure compared to Fig. 6. The results show that the dereverberation performance of all the methods degrade when a background noise is added to the reverberant microphone signals. As can be seen in Fig. 7, the best performance is obtained using the N-CTF+NMF and N-CTF+NMF+OC methods. These experiments show that the proposed methods are quite robust to the presence of background noise, and that even in the noisy scenarios, the proposed methods result in higher scores for the dereverberated speech signals compared to the baseline N-CTF and SE methods. It is important to note that we have not explicitly modeled the background noise in the proposed methods. This can be an interesting extension of the current methods, where Eq. (5) is modified such that the background noise is also explicitly modeled, e.g., using a separate NMF model.

C. Weighted Method

In this section the performance of the proposed integrated and weighted methods is compared, where no background noise is present. Fig. 8, Fig. 9, and Fig. 10 show the Δ PESQ, Δ CD, and Δ RDT obtained using the integrated and weighted methods as a function of the weighting parameter ρ for different RIRs. These figures compare the performance of three variants of the integrated method (N-CTF+NMF, N-CTF+NMF+LR, and N-CTF+NMF+OC) to the performance of the same variants of the weighted method, which are identified by the suffix '(w)'.

Results show that an optimal value for the weighting parameter ρ (denoted by ρ^*) can be found, using which the

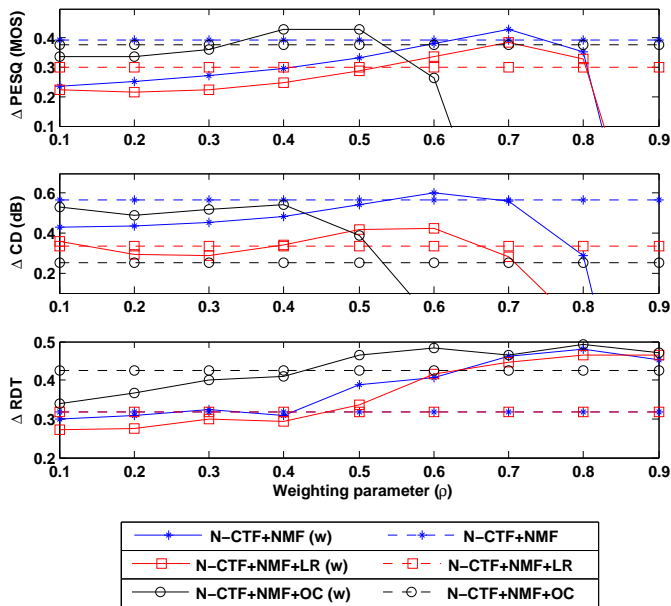


Fig. 8: Instrumental measures for the proposed integrated and weighted methods for a RIR with $T_{60} \approx 640$ ms and $DRR \approx 12$ dB.

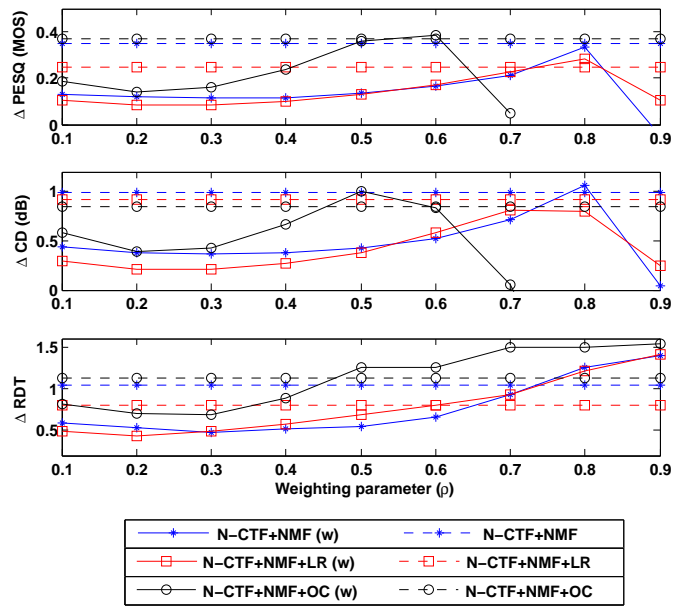


Fig. 10: Instrumental measures for the proposed integrated and weighted methods for a RIR with $T_{60} \approx 680$ ms and $DRR \approx 0$ dB.

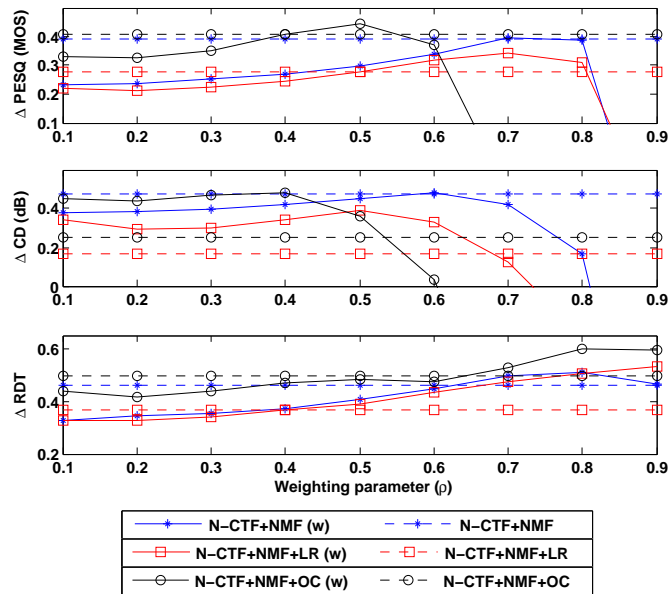


Fig. 9: Instrumental measures for the proposed integrated and weighted methods for a RIR with $T_{60} \approx 430$ ms and $DRR \approx 5$ dB.

obtained Δ PESQ for the weighted methods is similar or slightly better than the obtained Δ PESQ for the integrated methods. However, the optimal weighting parameter ρ^* depends on the considered RIR and the variant of the weighted method, i.e. the utilized NMF model. The results also show that the Δ CD measure is substantially higher for the N-CTF+NMF+OC (w) method using the optimal ρ^* compared to the N-CTF+NMF+OC method, while the two methods result in similar Δ RDT values. Moreover, using the optimal ρ^* , the obtained Δ CD and Δ RDT values using the N-CTF+NMF (w)

and N-CTF+NMF+LR (w) methods are similar to the Δ CD and Δ RDT values obtained using the N-CTF+NMF and N-CTF+NMF+LR methods.

Although it is possible to achieve a better dereverberation performance using the weighted method, the experiments show that the optimal weighting parameter ρ^* highly depends on both the room acoustics as well as the NMF spectral model, which is a disadvantage compared to the integrated method. It can be seen that for the N-CTF+NMF+OC (w) method, ρ^* is around 0.4 – 0.5, while for the N-CTF+NMF (w) and N-CTF+NMF+LR (w) methods, ρ^* is around 0.7 – 0.8. By increasing the value of ρ , a lower reverberant tail, i.e., higher Δ RDT, and a larger spectral distance, i.e., lower Δ CD, are typically achieved. This is more notable when an overcomplete NMF basis matrix \mathbf{W} is learned (N-CTF+NMF+OC (w)). This may be explained by noting that, in this case, the columns of \mathbf{W} are sampled from the spectrograms of the speaker-independent training clean speech signals. Therefore, each spectral vector of the dereverberated speech signal is approximated using very few, strictly speaking only one, columns of \mathbf{W} . This leads to a large value for the NMF cost function P in (20), and accordingly a relatively small ρ leads to the best dereverberation performance. For larger values of ρ (especially when $\rho > 0.8$) an estimate of the clean speech spectrogram is obtained that is a combination of the clean spectral vectors, and hence, a higher Δ RDT value is obtained. At the same time, since a lower weight is given to the acoustic cost function Q in (20), the obtained estimate of the clean speech spectrogram is highly distorted because it is largely independent of the observed signal.

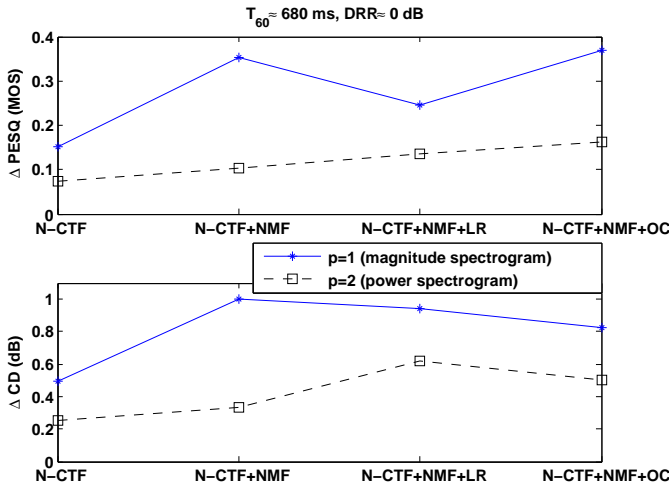


Fig. 11: Dereverberation performance using magnitude spectrogram ($p = 1$) and power spectrogram ($p = 2$).

D. Influence of the Parameters

In this section the influence of different parameters on the speech dereverberation performance in the absence of background noise is investigated. First, experiments show that the parameter p , which determines whether magnitude or power spectrograms are used, has a significant effect on the performance. Additionally, the number of iterations for the update rules and the STFT frame length were found to be quite influential. The effect of these parameters on the performance of the integrated method is separately studied, where only one parameter is varied and the other parameters are set to the values mentioned in Section V-A, i.e., $p = 1$ (magnitude spectrogram), frame length = 64 ms, and number of iterations = 20. The experiments in this section are performed for the RIR with $T_{60} \approx 680$ ms and DRR ≈ 0 dB, but similar observations were made for the other RIRs.

1) Magnitude versus power spectrogram. Fig. 11 shows Δ PESQ and Δ CD for power and magnitude spectrograms using the integrated methods. As can be clearly seen, a better performance is obtained using the magnitude spectrogram for all variants, even though the N-CTF model in (5) can theoretically be better justified using the power spectrogram. However, a similar observation has already been also made in NMF-based source separation and speech enhancement [31].

2) Number of iterations. Fig. 12 shows Δ PESQ and Δ CD as a function of the number of iterations, where the number of iterations $\in \{5, 10, 20, 50\}$. Results show that a small number of iterations (in the range of 5-20) is enough to obtain the best dereverberation performance.

3) Frame length. Fig. 13 shows Δ PESQ and Δ CD as a function of the STFT frame length, where the frame length $\in \{8, 16, 32, 64, 128\}$ ms and 50%-overlapping square-root Hann windows are used for all cases. As can be seen, the performance degrades significantly when shorter frames are used. The best performance is obtained when the frame length is around 64 ms.

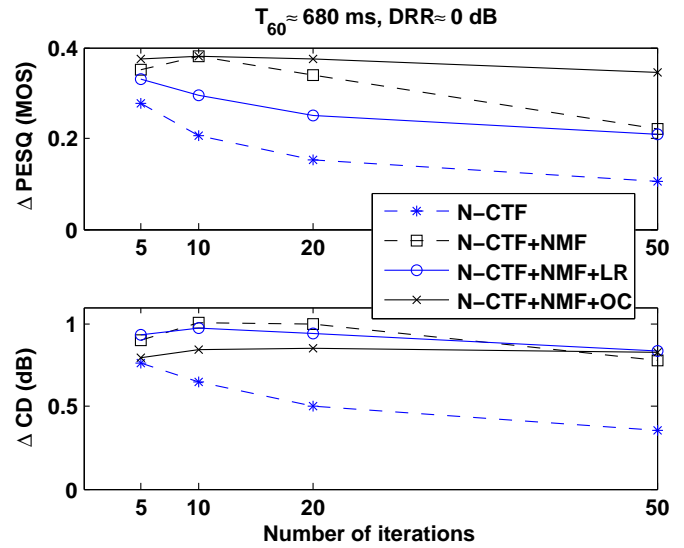


Fig. 12: Dereverberation performance as a function of the number of iterations.

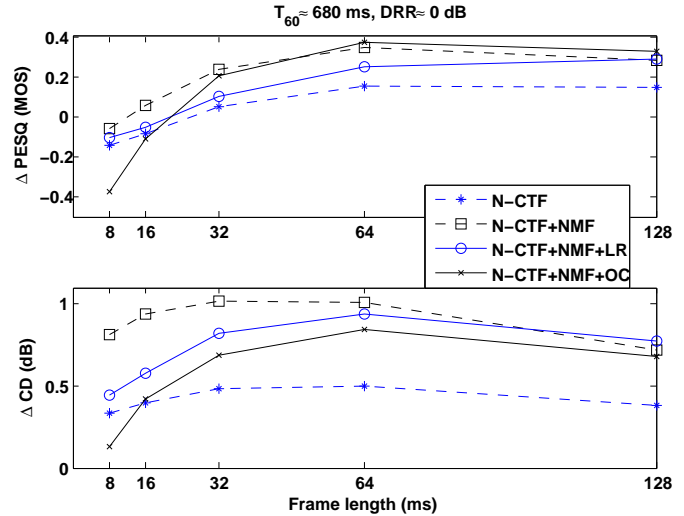


Fig. 13: Dereverberation performance as a function of the STFT frame length using 50% overlapping square-root Hann windows.

VI. CONCLUSION

In this paper, we have considered single-channel speech dereverberation methods combining an N-CTF-based acoustic model and an NMF-based spectral model in order to jointly exploit the room acoustics and speech spectral structure. Two methods are presented to combine the N-CTF and NMF models, namely the integrated method, where the NMF model is directly integrated into the N-CTF model, and the weighted method, where the N-CTF and NMF cost functions are weighted and summed. For both methods, generalized Kullback-Leibler divergence is used to define the cost functions and iterative update rules are derived to estimate the clean speech spectrogram.

Experimental results, with and without background noise, for three different RIRs showed that the performance of

the N-CTF-based dereverberation method was significantly improved by additionally exploiting the NMF-based spectral model, where considerably better-quality speech signals were obtained using the magnitude spectrograms compared to the power spectrograms. It was shown that the integrated method outperforms a state-of-the-art spectral enhancement method by 0.25 PESQ-MOS points. Results also showed that using the weighted method it is possible to achieve even a better performance, but that the optimal weighting parameter highly depends on the NMF model as well as the room acoustics. Using temporal dependencies based on a frame-stacking method was found to be useful only for highly reverberant conditions when a low-rank NMF basis matrix was learned offline from clean speech training data.

APPENDIX A

ASSUMPTIONS UNDERLYING THE N-CTF MODEL

Assuming that the phases of $h_c(k, \tau)$ at different frames are mutually independent uniformly-distributed random variables, (3) leads to [16]:

$$E\left(|y_c(k, t)|^2\right) \approx \sum_{\tau=0}^{L_h-1} |h_c(k, \tau)|^2 |s_c(k, t - \tau)|^2, \quad (35)$$

where $E(\cdot)$ denotes the mathematical expectation operator, and $|\cdot|$ denotes absolute value operator. Although this assumption about the phase may seem unrealistic, it is interesting to note that a similar expression has also been used in other state-of-the-art methods, such as [6], to relate the spectral variance of the reverberant speech signal to the spectral variance of the clean speech signal. In [6], assuming an exponential-decay model for the complex-valued RIR spectral coefficients $h_c(k, \tau)$, and assuming that $h_c(k, \tau)$ at different frames are mutually independent and zero-mean random variables with Gaussian distributions, it is shown that

$$E\left(|y_c(k, t)|^2\right) \approx \sum_{\tau=0}^{\infty} E\left(|h_c(k, \tau)|^2\right) E\left(|s_c(k, t - \tau)|^2\right), \quad (36)$$

where it is additionally assumed that the speech spectral coefficients $s_c(k, t)$ are independent and identically distributed zero-mean complex random variables with a certain distribution, and that the speech and the RIR spectral coefficients $s_c(k, t)$ and $h_c(k, \tau)$ are mutually independent.

Expression (35) is similar to (36) in that they both describe the spectral variance of the reverberant speech signal as a convolution of two non-negative signals, which are related to the magnitude-squared RIR and speech spectral coefficients $|h_c(k, \tau)|^2$ and $|s_c(k, t)|^2$. These expression differ in that instantaneous magnitude-squared coefficients are used in (35) while expected magnitude-squared coefficients are used in (36).

APPENDIX B

ITERATIVE LEARNING USING AUXILIARY FUNCTIONS

Iterative learning is a commonly used method to minimize a cost function with non-negativity constraints. This section provides a brief review of an iterative learning method based on the auxiliary function method [21] that is used in this paper.

Consider a cost function $Q(h, s)$, where the unknown parameters h and s are constrained to be non-negative. Using the auxiliary function method, we can derive an iterative method to minimize $Q(h, s)$ in order to obtain an estimate for h and s . Let i denote the iteration index, and h^i and s^i denote the estimates of h and s at the i -th iteration, respectively. The main idea behind the iterative learning method using an auxiliary function is the following lemma from [21]:

Lemma 1: Let $G(h, h^i)$ be an auxiliary function for the cost function $L(h)$ such that $G(h, h) = L(h)$ and $G(h, h^i) \geq L(h)$ for a given h^i and for all h . Let h^{i+1} be the new estimate obtained by minimizing $G(h, h^i)$ with respect to (w.r.t.) h . $L(h)$ is non-increasing under this update, i.e., $L(h^{i+1}) \leq L(h^i)$, where the equality only holds when h^i is a local minimum of $L(h)$.

Considering our problem to minimize $Q(h, s)$, an update rule for h can be derived as follows: assuming that h^i and s^i are given, h^{i+1} can be computed by minimizing $L(h) = Q(h, s^i)$ w.r.t. h . This is done in two steps: in the first step, an auxiliary function $G(h, h^i)$ is obtained for $L(h)$. In the second step, the auxiliary function $G(h, h^i)$ is differentiated w.r.t. h , and the derivative is set to zero, leading to a new value for h , referred to as h^{i+1} , which is a function of h^i , s^i , and all the other known parameters. The method is now continued to compute s^{i+1} given h^{i+1} and s^i . These iterations are executed until a local minimum of the cost function $Q(h, s)$ is obtained. Note that this iterative method can be trivially extended to minimize a function with more than two unknown parameters.

A useful inequality that is often used to obtain an auxiliary function is stated in the following lemma from [21]:

Lemma 2: If $\phi(x)$ is a convex function and a_τ are non-negative coefficients for which $\sum_\tau a_\tau = 1$, Jensen's inequality [42] can be used to derive the following inequality:

$$\phi\left(\sum_\tau x_\tau\right) \leq \sum_\tau a_\tau \phi\left(\frac{x_\tau}{a_\tau}\right). \quad (37)$$

APPENDIX C

MODELING TEMPORAL DEPENDENCIES IN THE INTEGRATED METHOD USING FRAME STACKING

Let $\mathbf{y}(t)$ denote the t -th column of \mathbf{Y} . We define the KT_{st} -dimensional stacked vector $\mathbf{y}_{st}(t)$ as $\mathbf{y}_{st}(t) = [\mathbf{y}^T(t) \dots \mathbf{y}^T(t+T_{st}-1)]^T$, where T denotes matrix transpose. The stacked vector $\mathbf{s}_{st}(t)$ is defined similarly, and the stacked vector $\mathbf{h}_{st}(t)$ is defined as $\mathbf{h}_{st}(t) = [\mathbf{h}^T(t) \dots \mathbf{h}^T(t)]^T$. Similarly to (13), a cost function based on the generalized KL divergence can now be defined as:

$$L_{1,st} = \lambda \sum_{r,t} x(r, t) + \sum_{l=1}^{T_{st}} \sum_{k,t} KL\left(\mathbf{y}_{st}(f_l, t) \left| \sum_{\tau=0}^{L_h-1} h_{st}(f_l, \tau) \sum_{r=1}^R w(f_l, r) x(r, t - \tau)\right.\right), \quad (38)$$

where $f_l = k + K(l - 1)$, and $\mathbf{W} = [w(f_l, r)]$ is a $KT_{st} \times R$ -dimensional matrix. The update rules for w and x remain identical to (15) and (16), where the update rule for h can be

derived as:

$$h^{i+1}(k, \tau) = h^i(k, \tau) \times \frac{\sum_{l=1}^{T_{st}} \sum_t y_{st}(f_l, t) \tilde{s}_{st}(f_l, t - \tau) / \tilde{y}_{st}(f_l, t)}{\sum_{l=1}^{T_{st}} \sum_t \tilde{s}_{st}(f_l, t - \tau)}, \quad (39)$$

where $\tilde{s}_{st}(f_l, t) = \sum_r w^i(f_l, r) x^i(r, t)$ and $\tilde{y}_{st}(f_l, t) = \sum_\tau h_{st}^i(f_l, \tau) \tilde{s}_{st}(f_l, t - \tau)$. By setting $T_{st} = 1$, (14) is obtained as a special case of (39).

After convergence of the iterations, the clean speech spectrogram is estimated as $\hat{s}(k, t) = G(k, t)y(k, t)$, where the time-varying gain function $G(k, t)$ is obtained by averaging the overlapping segments, i.e.

$$G(k, t) = \frac{\sum_{l=1}^{T_{st}} \sum_r \hat{w}(f_l, r) \hat{x}(r, t)}{\sum_{l=1}^{T_{st}} \sum_{r, \tau} \hat{h}_{st}(f_l, \tau) \hat{w}(f_l, r) \hat{x}(r, t - \tau)}, \quad (40)$$

where $\hat{(\cdot)}$ is used to denote the obtained estimates after convergence, and the KT_{st} -dimensional vector $\mathbf{h}_{st}^i(t)$ is defined as $\mathbf{h}_{st}^i(t) = [\mathbf{h}^{i,T}(t) \dots \mathbf{h}^{1,T}(t)]^T$. As can be seen, (40) reduces to (18) when $T_{st} = 1$.

C:/Nasser/ASLP2015 N-CTF based Dereverb/NasserRefs

REFERENCES

- [1] P. A. Naylor and N. D. Gaubitch, Eds., *Speech Dereverberation*, 1st ed. New York, USA: Springer, 2010.
- [2] R. Beutelmann and T. Brand, "Prediction of speech intelligibility in spatial noise and reverberation for normal-hearing and hearing-impaired listeners," *Journal of Acoustical Society of America (JASA)*, vol. 120, no. 1, pp. 331–342, Jul. 2006.
- [3] J. B. Allen, D. A. Berkley, and J. Blauert, "Multimicrophone signal-processing technique to remove room reverberation from speech signals," *Journal of Acoustical Society of America (JASA)*, vol. 62, no. 4, pp. 912–915, 1977.
- [4] K. Lebart, J. M. Bouche, and P. N. Denbigh, "A new method based on spectral subtraction for speech dereverberation," *Acta Acoustica*, vol. 87, no. 3, pp. 359–366, 2001.
- [5] E. A. P. Habets, "Single- and multi-microphone speech dereverberation using spectral enhancement," Ph.D. dissertation, Technische Universiteit Eindhoven, Eindhoven, The Netherlands, 2007.
- [6] E. A. P. Habets, S. Gannot, and I. Cohen, "Late reverberant spectral variance estimation based on a statistical model," *IEEE Signal Process. Letters*, vol. 16, no. 9, pp. 770–773, Sep. 2009.
- [7] A. Kuklasieński, S. Doclo, T. Gerkmann, S. H. Jensen, and J. Jensen, "Multi-channel PSD estimators for speech dereverberation - A theoretical and experimental comparison," in *Proc. IEEE Int. Conf. Acoustics, Speech, and Signal Process. (ICASSP)*, Brisbane, Australia, Apr. 2015, pp. 91–95.
- [8] A. Schwarz and W. Kellermann, "Coherent-to-diffuse power ratio estimation for dereverberation," *IEEE/ACM Trans. on Audio, Speech and Language Process.*, vol. 23, no. 6, pp. 1006–1018, 2015.
- [9] T. Nakatani, T. Yoshioka, K. Kinoshita, M. Miyoshi, and J. Biing-Hwang, "Speech dereverberation based on variance-normalized delayed linear prediction," *IEEE Trans. Audio, Speech, and Language Process.*, vol. 18, no. 7, pp. 1717–1731, Sep. 2010.
- [10] A. Jukić and S. Doclo, "Speech dereverberation using weighted prediction error with Laplacian model of the desired signal," in *Proc. IEEE Int. Conf. Acoustics, Speech, and Signal Process. (ICASSP)*, Florence, Italy, May 2014, pp. 5172–5176.
- [11] D. Schmid, G. Enzner, S. Malik, D. Kolossa, and R. Martin, "Variational Bayesian inference for multichannel dereverberation and noise reduction," *IEEE/ACM Transactions on Audio, Speech, and Language Process.*, vol. 22, no. 8, pp. 1320–1335, Aug. 2014.
- [12] M. Miyoshi and Y. Kaneda, "Inverse filtering of room acoustics," *IEEE Transactions on Acoustics, Speech and Signal Process.*, vol. 36, no. 2, pp. 145–152, Feb. 1988.
- [13] Y. A. Huang and J. Benesty, "A class of frequency-domain adaptive approaches to blind multichannel identification," *IEEE Trans. Signal Process.*, vol. 51, no. 1, pp. 11–24, Jan. 2003.
- [14] F. Lim, Z. Wancheng, E. A. P. Habets, and P. A. Naylor, "Robust multichannel dereverberation using relaxed multichannel least squares," *IEEE/ACM Transactions on Audio, Speech, and Language Processing*, vol. 22, no. 9, pp. 1379–1390, Sep. 2014.
- [15] I. Kodrasi, S. Goetze, and S. Doclo, "Regularization for partial multichannel equalization for speech dereverberation," *IEEE Trans. Audio, Speech, and Language Process.*, vol. 21, no. 9, pp. 1879–1890, Sep. 2013.
- [16] H. Kameoka, T. Nakatani, and T. Yoshioka, "Robust speech dereverberation based on non-negativity and sparse nature of speech spectrograms," in *Proc. IEEE Int. Conf. Acoustics, Speech, and Signal Process. (ICASSP)*, Taipei, Taiwan, Apr. 2009, pp. 45–48.
- [17] R. Singh, B. Raj, and P. Smaragdis, "Latent-variable decomposition based dereverberation of monaural and multi-channel signals," in *Proc. IEEE Int. Conf. Acoustics, Speech, and Signal Process. (ICASSP)*, Dallas, Texas, USA, Mar. 2010, pp. 1914–1917.
- [18] K. Kumar, "A spectro-temporal framework for compensation of reverberation for speech recognition," Ph.D. dissertation, Dept. of ECE, Carnegie Mellon University, Pittsburgh, USA, 2011.
- [19] M. Yu and F. K. Soong, "Constrained multichannel speech dereverberation," in *Proc. Int. Conf. Spoken Language Process. (Interspeech)*, Portland, Oregon, USA, 2012.
- [20] H. Kallasjoki, J. F. Gemmeke, K. J. Palomäki, A. V. Beeston, and G. J. Brown, "Recognition of reverberant speech by missing data imputation and NMF feature enhancement," in *Proc. REVERB workshop*, Florence, Italy, May 2014.
- [21] D. D. Lee and H. S. Seung, "Algorithms for non-negative matrix factorization," in *Advances in Neural Information Process. Systems (NIPS)*. MIT Press, 2000, pp. 556–562.
- [22] A. Cichocki, R. Zdunek, A. H. Phan, and S. Amari, *Nonnegative Matrix and Tensor Factorizations: Applications to Exploratory Multi-way Data Analysis and Blind Source Separation*. New York: John Wiley & Sons, 2009.
- [23] P. Smaragdis, B. Raj, and M. V. Shashanka, "A probabilistic latent variable model for acoustic modeling," in *Advances in Models for Acoustic Process. Workshop, NIPS*. MIT Press, 2006.
- [24] T. Virtanen, "Monaural sound source separation by non-negative matrix factorization with temporal continuity and sparseness criteria," *IEEE Trans. Audio, Speech, and Language Process.*, vol. 15, no. 3, pp. 1066–1074, 2007.
- [25] C. Févotte, N. Bertin, and J. L. Durrieu, "Nonnegative matrix factorization with the Itakura-Saito divergence: with application to music analysis," *Neural Computation*, vol. 21, pp. 793–830, 2009.
- [26] J. F. Gemmeke, T. Virtanen, and A. Hurmalainen, "Exemplar-based sparse representations for noise robust automatic speech recognition," *IEEE Trans. Audio, Speech, and Language Process.*, vol. 19, no. 7, pp. 2067–2080, Sep. 2011.
- [27] N. Mohammadiha, P. Smaragdis, and A. Leijon, "Supervised and unsupervised speech enhancement using NMF," *IEEE Trans. Audio, Speech, and Language Process.*, vol. 21, no. 10, pp. 2140–2151, Oct. 2013.
- [28] N. Mohammadiha, P. Smaragdis, and S. Doclo, "Joint acoustic and spectral modeling for speech dereverberation using non-negative representations," in *Proc. IEEE Int. Conf. Acoustics, Speech, and Signal Process. (ICASSP)*, Brisbane, Australia, Apr. 2015.
- [29] Y. Avargel and I. Cohen, "System identification in the short-time Fourier transform domain with crossband filtering," *IEEE Trans. Audio, Speech, and Language Process.*, vol. 15, no. 4, pp. 1305–1319, May 2007.
- [30] R. Talmon, I. Cohen, and S. Gannot, "Relative transfer function identification using convolutive transfer function approximation," *IEEE Trans. Audio, Speech, and Language Process.*, vol. 17, no. 4, pp. 546–555, May 2009.
- [31] N. Mohammadiha, "Speech enhancement using nonnegative matrix factorization and hidden Markov models," Ph.D. dissertation, KTH - Royal Institute of Technology, Stockholm, Sweden, 2013. [Online]. Available: <http://theses.eurasip.org/theses/499/speech-enhancement-using-nonnegative-matrix/download/>
- [32] N. Mohammadiha, P. Smaragdis, G. Panahandeh, and S. Doclo, "A state-space approach to dynamic nonnegative matrix factorization," *IEEE Trans. Signal Process.*, vol. 63, no. 4, pp. 949–959, Feb. 2015.
- [33] R. Corless, G. Gonnet, D. Hare, D. Jeffrey, and D. Knuth, "On the Lambert W function," *Advances in Computational Mathematics*, vol. 5, pp. 329–359, 1996.
- [34] J. S. Garofolo, L. F. Lamel, W. M. Fisher, J. G. Fiscus, D. S. Pallett, and N. L. Dahlgren, "TIMIT acoustic-phonetic continuous speech corpus." Philadelphia: Linguistic Data Consortium, 1993.

- [35] I.-T. P.862, "Perceptual evaluation of speech quality (PESQ), and objective method for end-to-end speech quality assesment of narrowband telephone networks and speech codecs," Tech. Rep., 2000.
- [36] Y. Hu and P. Loizou, "Evaluation of objective quality measures for speech enhancement," *IEEE Trans. Audio, Speech, and Language Process.*, vol. 16, no. 1, pp. 229–238, Jan 2008.
- [37] J. Y. C. Wen and P. A. Naylor, "An evaluation measure for reverberant speech using decay tail modelling," in *Proc. European Signal Process. Conf. (EUSIPCO)*, Florence, Italy, Sep. 2006.
- [38] S. Goetze, A. Warzybok, I. Kodrasi, J. O. Jungmann, B. Cauchi, J. Rennie, E. Habets, A. Mertins, T. Gerkmann, S. Doclo, and B. Kollmeier, "A study on speech quality and speech intelligibility measures for quality assessment of single-channel dereverberation algorithms," in *Proc. Int. Workshop on Acoust. Echo and Noise Control (IWAENC)*, Antibes, France, Sep. 2014, pp. 234–238.
- [39] N. Mohammadiha and S. Doclo, "Single-channel dynamic exemplar-based speech enhancement," in *Proc. Int. Conf. Spoken Language Process. (Interspeech)*, Singapore, Sep. 2014, pp. 2690–2694.
- [40] A. Cichocki, R. Zdunek, and S. Amari, "New algorithms for non-negative matrix factorization in applications to blind source separation," in *Proc. IEEE Int. Conf. Acoustics, Speech, and Signal Process. (ICASSP)*, vol. 5, Toulouse, France, May 2006.
- [41] Y. Ephraim and D. Malah, "Speech enhancement using a minimum mean-square error log-spectral amplitude estimator," *IEEE Trans. Acoust., Speech, Signal Process.*, vol. 33, no. 2, pp. 443–445, Apr. 1985.
- [42] C. R. Rao, *Linear Statistical Inference and Its Applications*, 2nd ed. New York: Wiley, 1973.